OMTN, Volume *17*

Supplemental Information

Development of a Monomeric Inhibitory RNA Aptamer Specific for FGFR3 that Acts as an Activator When Dimerized

Nachiket Kamatkar, Matthew Levy, and Jean M. Hébert

Supplementary Materials

Supplementary Table 1. Selection parameters for rounds 1-10.

Round	# of cycles LS-PCR*	Input RNA (pmol)**	Type	
1	14	1000	5 µg	Recom-binant Protein
2	16	100	5 µg	
3	16	100	0.5 µg	
4	16	100	0.5 µg	
5	16	100	0.5 µg	
6	16	100	0.5 µg	
7	24	100	N2A only	Cells
8	24	100	3T3→N2A	
9	27	100	3T3→N2A (cell internalization)	
10	26	100	3T3→N2A (cell internatization)	

*Number of large-scale PCR cycles, amount of input RNA, and whether the round was performed on mouse FGFR3c extracellular domain (rounds 1-6) or FGFR3-expressing Neuro2A (N2A) cells (rounds 7-10). **Note that the amount of input RNA was decreased in the second round and the amount of protein was dropped by a tenth during round 3.

Supplementary Figure 1. Analysis of rounds 7-10.

(A) Rounds 7 through 10 of the selection display a significant shift when compared to resin and the reverse oligo controls. However, compared to round 6, the shift was minimal in the later rounds. **(B)** Individual clones from round 10 also bound both mouse and human FGFR3c. R10c35 on mouse FGFR3c; R10c35 on human FGFR3c; R10c12 on mouse FGFR3c; R10c12

on human FGFR3c. **(C)** Western blot of Neuro2A cells, but not NIH3T3 cells, shows expression of FGFR3. **(D)** BaF3 cells electroporated with BaF3-FGFR3b (mouse) do not grow after a 72 hour incubation with 0.4 nM FGF2. **(E)** BaF3 R3c:R1c cells grown for 48 hr and 72 hr with 0.4 nM FGF2 with 4 different seeding densities.

Supplementary Figure 2. Competition of aptamers from round 6 and round 10.

(A) Predicted secondary structure of NK01 illustrates the unused forward region and the long stem that were subsequently minimized during synthesis of NK01.min1 and iR3. Arrow heads indicate the theoretical primary loops used for binding. **(B)** The two dominant folds of iR3 are retained from the parent molecule and are most likely in equilibrium in solution. **(C)** Inhibition of growth of BaF3-R3c:R1c after 72 hours in 0.4 nM FGF2 by different chemically synthesized minimized constructs including iR3. All the constructs display comparable inhibition at higher concentrations of the aptamer.

Supplementary Figure 3. Binding of iR3 to parental and engineered BaF3 cell lines.

(A-C) iR3 and ctrl.36 were analyzed for binding to parental and engineered BaF3 cells at a concentration of 200 nmol/l. A significant shift was observed with iR3 only when incubated with BaF3-R3b and BaF3-R3c:R1c cells while only minor staining was observed when iR3 was

incubated with the parental BaF3 cell line. **(D)** Binding curves of labeled iR3 to mouse and human FGFR3b protein display the calculated apparent Kd of ~62 and ~48 nmol/l, which is similar to mouse and human FGFR3c (Figure 3B).

Supplementary Figure 4. FGF2 and iR3 compete for binding to FGFR3

Competition experiments were carried out using a constant concentration of Dylight650 labeled iR3 at 20 nM and increasing concentrations of FGF2. At higher FGF2 concentrations, iR3 is prevented from binding to both mouse and human FGFR3, indicated by a stark reduction in fluorescence (background fluorescence subtracted).

Supplementary Figure 5. Bivalent aptamer of iR3 with different uridine linker lengths.

(A) Binding of different uridine (1U, 3U, or 5U) linker clones and the parent clone R6c6 to mouse and human FGFR3c at a concentration of 100 nmol/l. Mouse FGFR3c is indicated in red and human FGFR3c in blue. **(B)** Predicted secondary structures of aR3. The 3' reverse primer region was excluded in the sequence analysis. Arrow heads indicate the theoretical primary loops used for binding. **(C)** Confirmation that aR3 stimulates BaF3-R3c:R1c cells with a titration of a different batch of this aptamer.

Supplementary Figure 6. Western blots of Cre- and Cre+ embryos.

(A-B) Western blot of cells from Cre negative control embryos, in which all three receptors are undeleted, stained for pERK indicating that iR3 does not inhibit signaling through FGFR1 or FGFR2. n=3 embryos. Cells only vs FGF2, p=0.0082; Cells only vs iR3+FGF2, p=0.0124; Cells only vs Ctrl.36+FGF2 p=0.0097. **(C-D)** Western blot of cells from,Cre positive control embryos, in which FGFR2 and FGFR3 are deleted and one allele of FGFR1 is left undeleted, indicates that iR3 does not inhibit FGF2 from binding FGFR1. n=5 embryos. Cells only vs FGF2, p=0.0079; Cells only vs iR3+FGF2, p=0.0059; Cells only vs Ctrl.36+FGF2; p= 0.0055. **(E-F)** Western blot of cells from,Cre positive control embryos, in which FGFR1 and FGFR3 are deleted and one allele of FGFR2 is left undeleted, indicates that iR3 does not inhibit FGF2 from binding FGFR2. n=3 embryos. Cells only vs FGF2, p=0.0376; Cells only vs iR3+FGF2, p=0.0261; Cells only vs Ctrl.36+FGF2; p= 0.0248. Together these experiments illustrate that iR3 binds and is specific for FGFR3 in a physiologically relevant context.

Supplementary Figure 7. Induction by FGF2 and inhibition by iR3 of pERK are similar over time.

Western blot analyses examining pERK induction by FGF2 (0.4 nM) and inhibition of induction by iR3 (1 uM) at 5, 10, 20, and 30 minute incubation times. Cells were first starved for 3 hours prior to the experiment. Values for pERK were normalized for ERK and are relative to the "+FGF2" sample. iR3 treatment similarly inhibit the FGF2 effect at all time points (for comparisons between FGF and FGF+iR3 samples: ***, $p = 0.0002$ (5 min) 0.0007 (10 min); ****, $p < 0.0001$, *, $p = 0.015$; 1-way ANOVA with multiple comparison with Dunnett correction; $N \geq 3$).

Supplementary Figure 8. Levels of pAKT and FGFR3 are unaffected by either FGF2 or aptamers.

(A) Western blot analysis of pAKT after addition of FGF2 (0.4 nM) and FGF2 + aptamers (1 uM) after X minutes in culture reveals no detectable effects. pAKT values were normalized to AKT levels and are relative to the +FGF2 sample. **(B)** Similarly, FGFR3 levels, normalized to βactin, were unaffected by FGF2 application or aptamers (1-way ANOVA with multiple comparison with Dunnett correction; N=3).

Supplementary Figure 9. BaF3 cells express physiological levels of the FGFR3:R1 chimera protein.

Western blot analysis using an anti-FGFR3 antibody against the N-terminus of FGFR3 revealed lower levels of receptor in BaF3 cells compared with astrocytic cells (mouse cortical astrocytes immortalized with hTERT). Values for FGFR3 were quantified on ImageJ and normalized to βactin. Unpaired two-tailed t-test, $p < 0.0001$.

Supplementary Figure 1

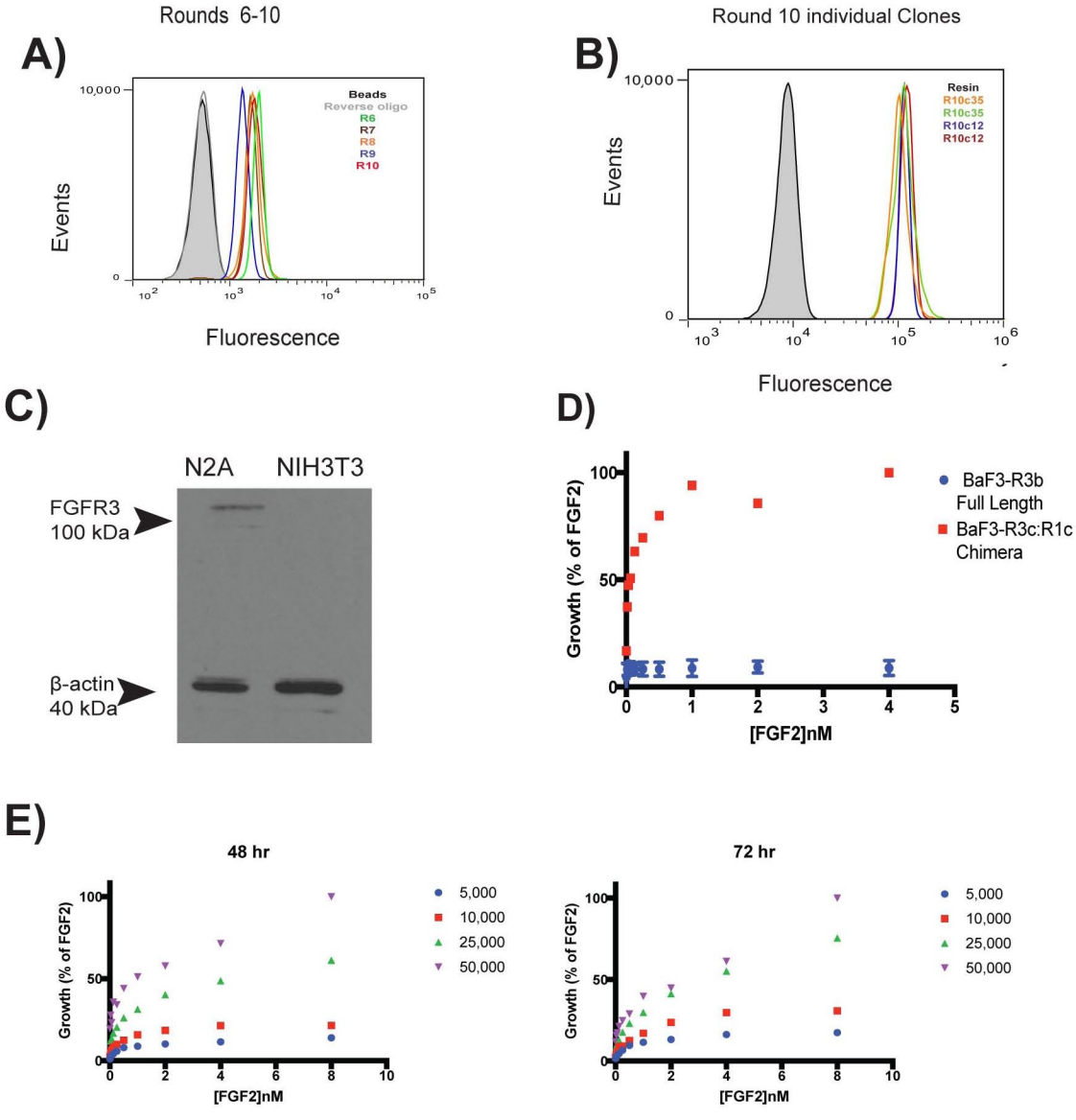

Supplementary Figure 2

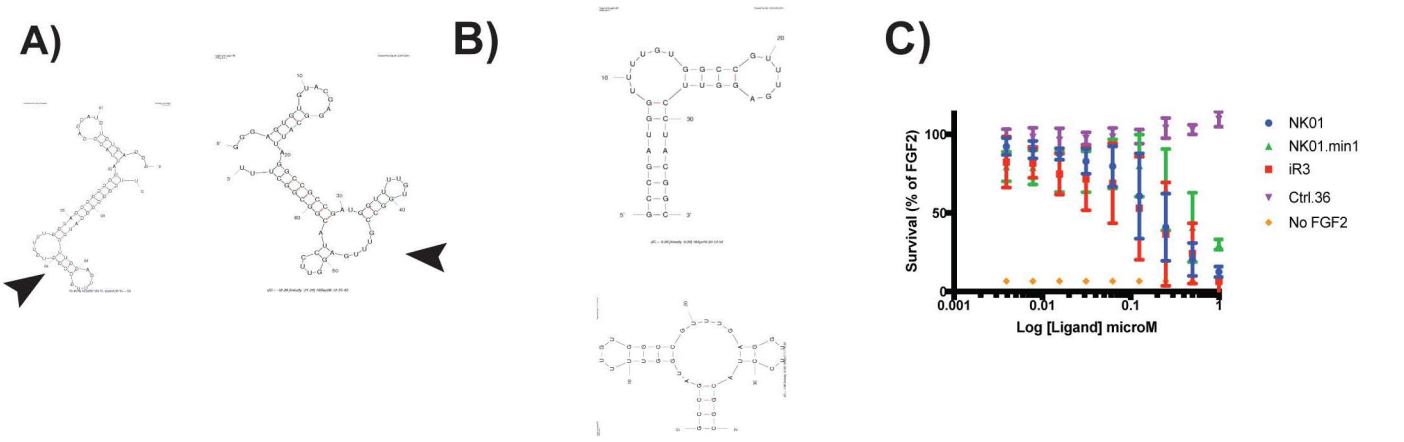

Supplementary Figure 3

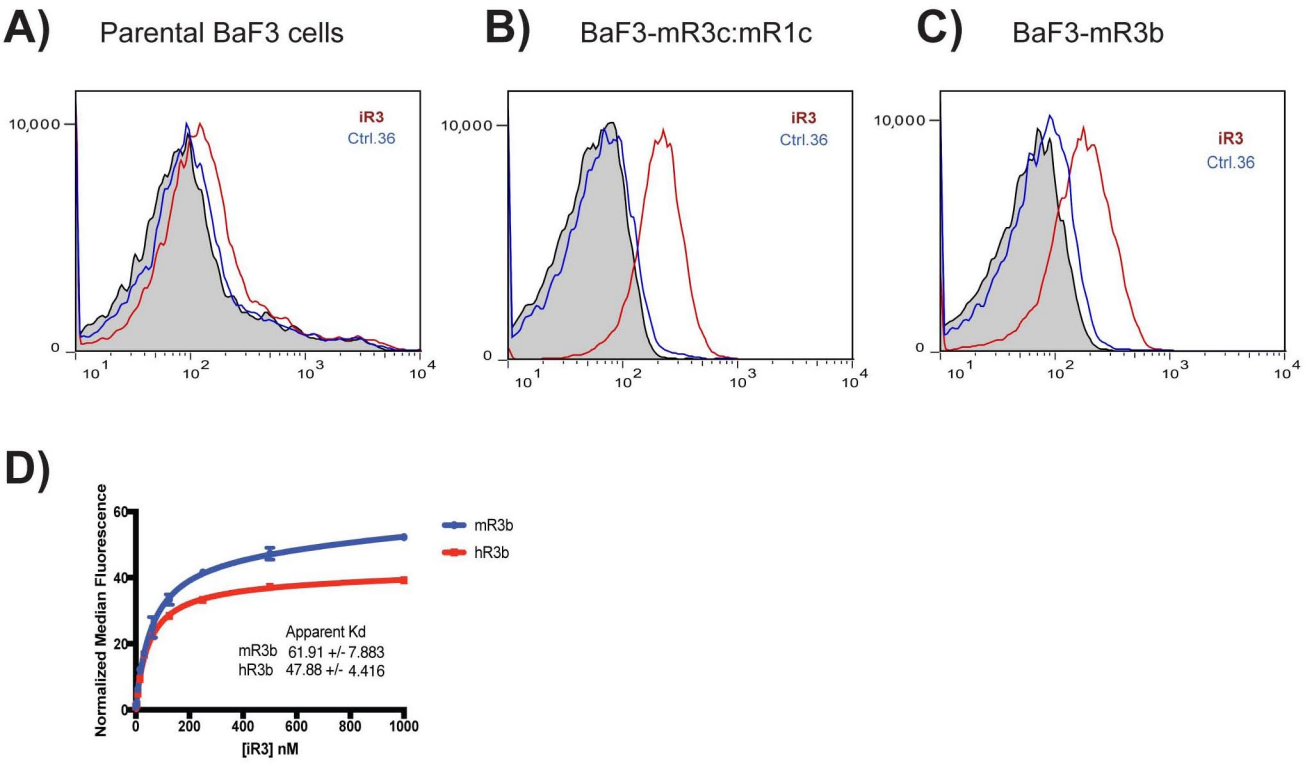

Supplementary Figure 4

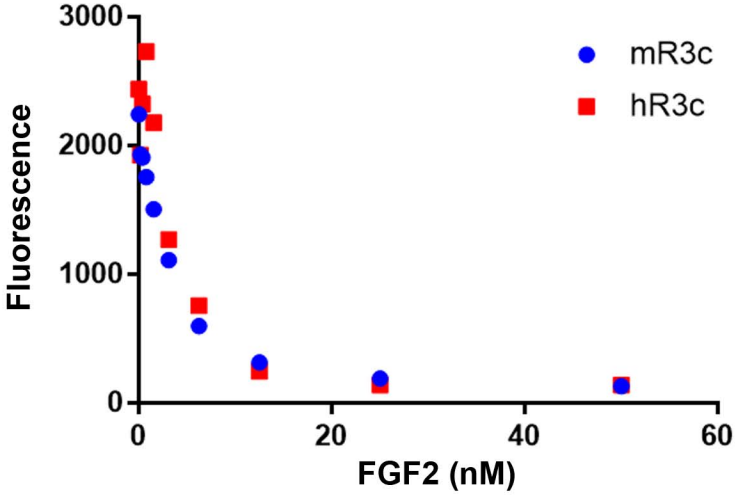

Supplementary Figure 5

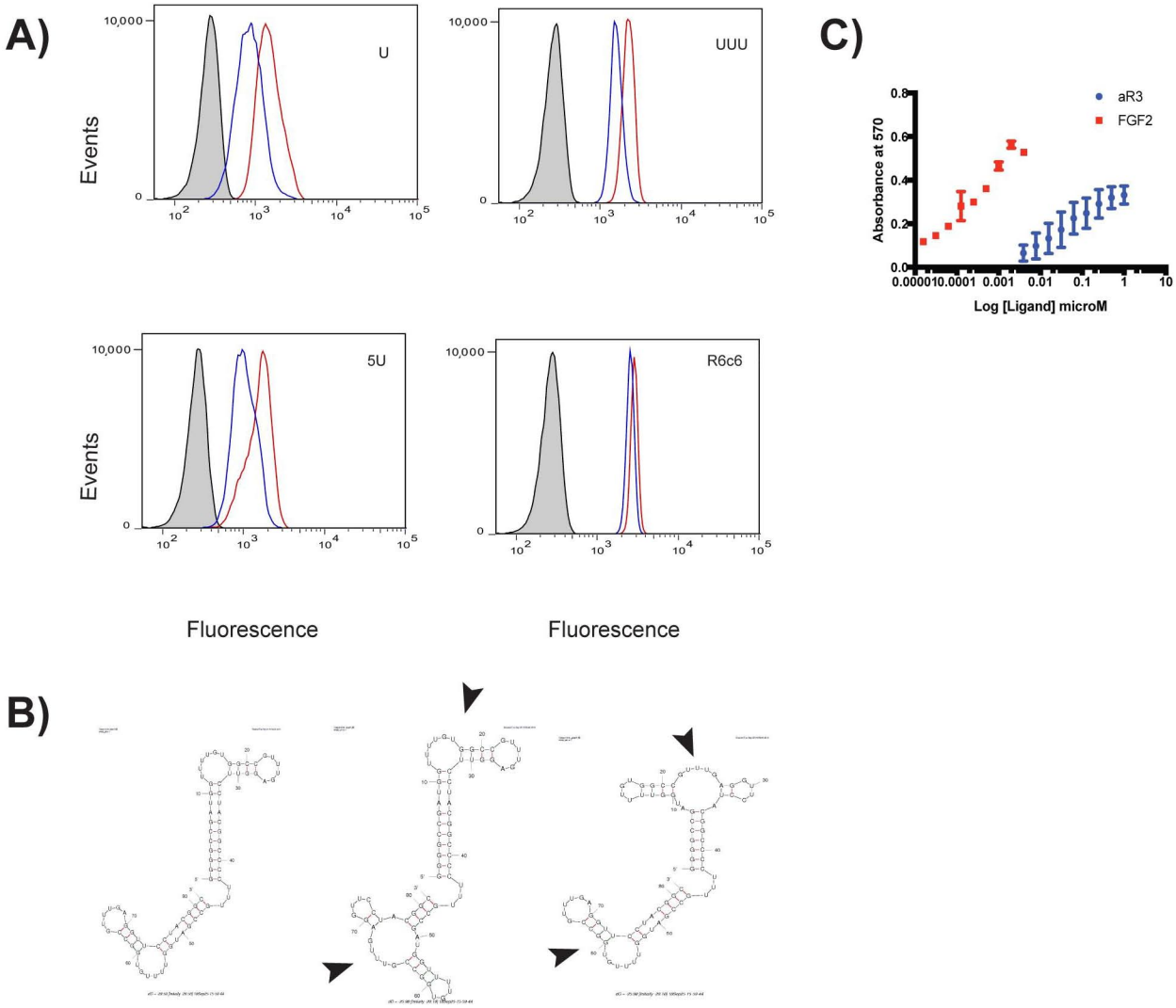

Supplementary Figure 6

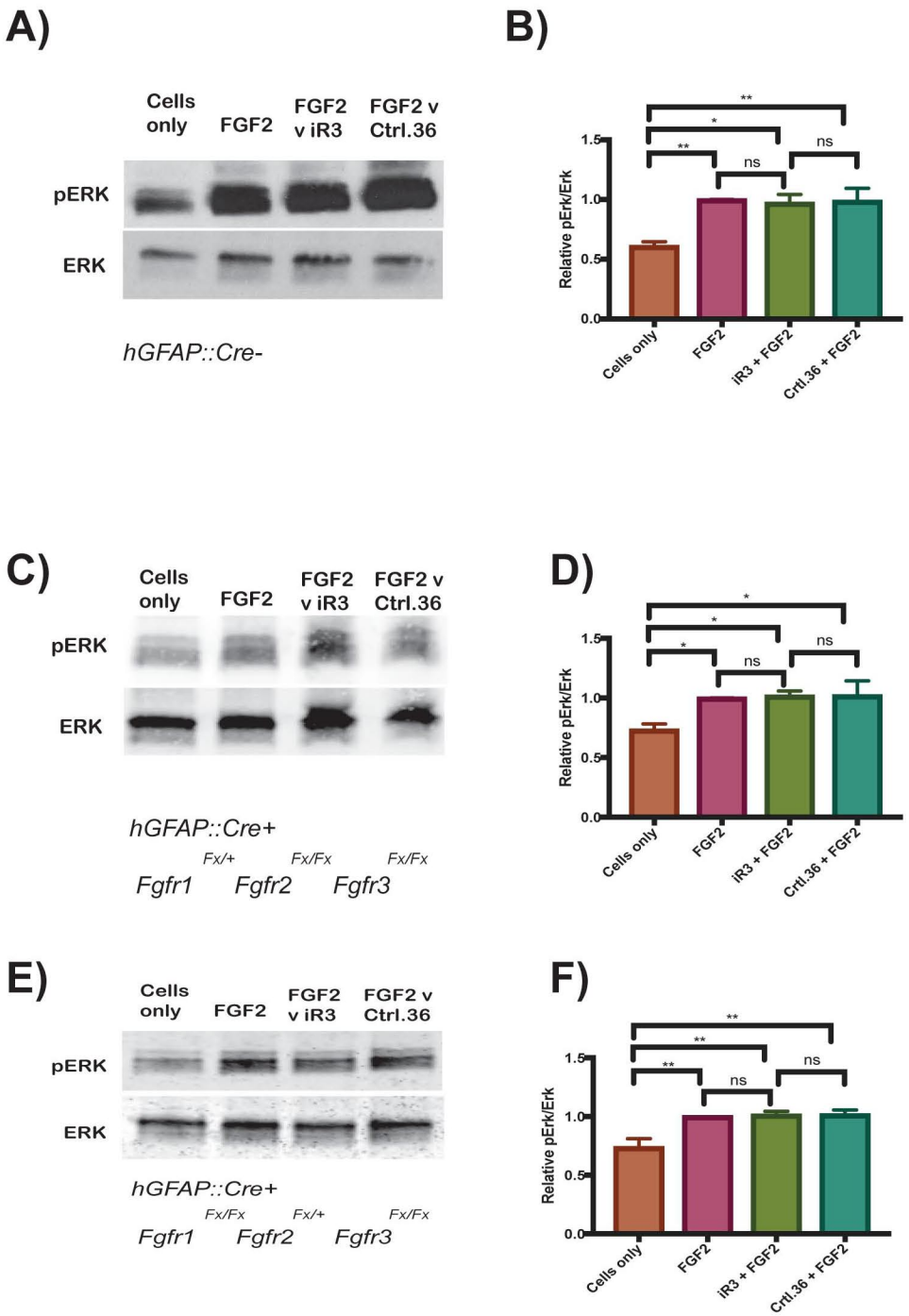

Supplementary Figure 7

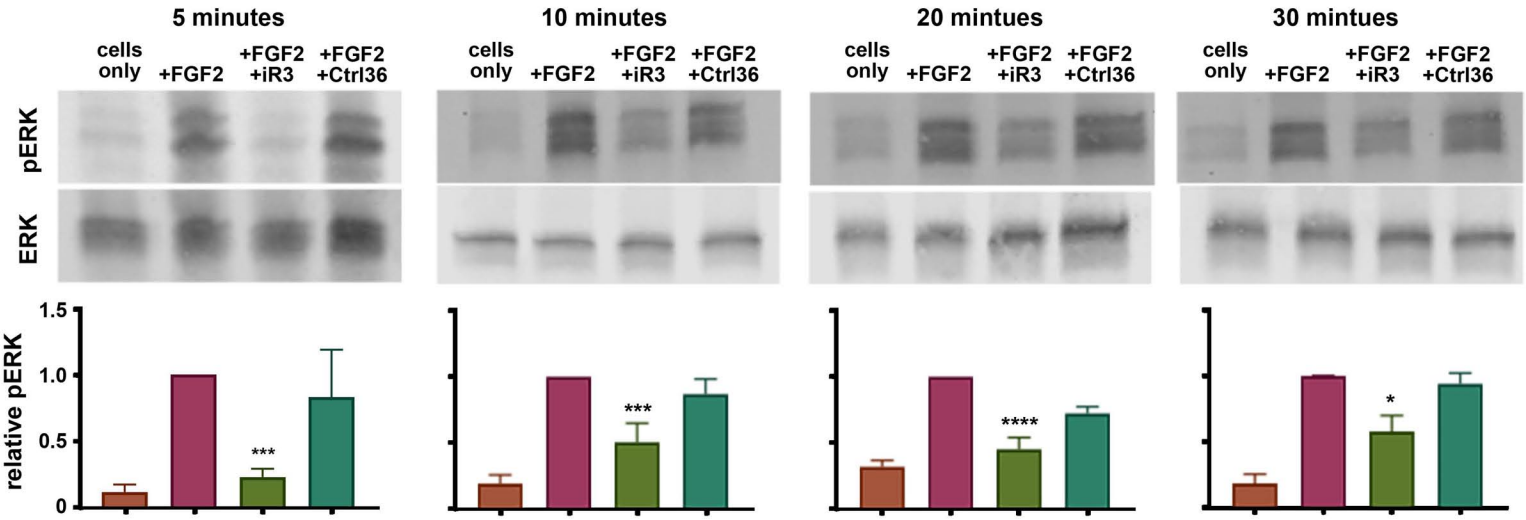

Supplementary Figure 8

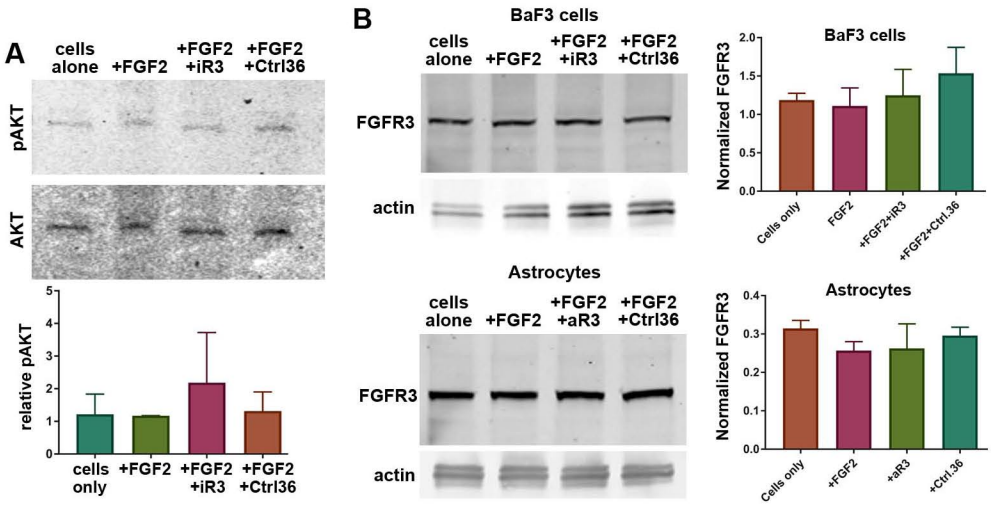

Supplementary Figure 9